

## Convergence Detection in Direct Simulation Monte Carlo Calculations for Steady State Flows

Jonathan M. Burt<sup>1,\*</sup> and Iain D. Boyd<sup>2</sup>

<sup>1</sup> U.S. Air Force Research Laboratory, Wright-Patterson Air Force Base, OH 45433, USA.

<sup>2</sup> Department of Aerospace Engineering, University of Michigan, 1320 Beal Avenue, Ann Arbor, MI 48109, USA.

Received 9 February 2010; Accepted (in revised version) 31 December 2010

Communicated by Rho Shin Myong

Available online 13 June 2011

---

**Abstract.** A new criterion is presented to detect global convergence to steady state, and to identify local transient characteristics, during rarefied gas flow simulations performed using the direct simulation Monte Carlo (DSMC) method. Unlike deterministic computational fluid dynamics (CFD) schemes, DSMC is generally subject to large statistical scatter in instantaneous flow property evaluations, which prevents the use of residual tracking procedures as are often employed in CFD simulations. However, reliable prediction of the time to reach steady state is necessary for initialization of DSMC sampling operations. Techniques currently used in DSMC to identify steady state convergence are usually insensitive to weak transient behavior in small regions of relatively low density or recirculating flow. The proposed convergence criterion is developed with the goal of properly identifying such weak transient behavior, while adding negligible computational expense and allowing simple implementation in any existing DSMC code. Benefits of the proposed technique over existing convergence detection methods are demonstrated for representative nozzle/plume expansion flow, hypersonic blunt body flow and driven cavity flow problems.

**AMS subject classifications:** 65C05, 76M28

**Key words:** Monte Carlo methods, particle methods, direct simulation Monte Carlo.

---

## 1 Introduction

The direct simulation Monte Carlo (DSMC) method [1] has been developed over the past several decades as a general simulation scheme for dilute gas flows with signifi-

---

\*Corresponding author. *Email addresses:* jonathan.m.burt@nasa.gov (J. M. Burt), iainboyd@umich.edu (I. D. Boyd)

cant translational nonequilibrium, and is commonly used to simulate a wide variety of rarefied flows. In contrast to typical computational fluid dynamics (CFD) schemes based on discrete approximations for a system of partial differential equations, DSMC employs Lagrangian particle tracking along with probabilistic collision procedures to replicate underlying physical processes in the governing Boltzmann equation. In DSMC simulations of steady state flows, output quantities of interest are typically sampled over a large number of time steps in order to reduce statistical scatter. For accurate results, sampling should be initiated only after steady state conditions have been realized across the entire simulated flowfield, following some transient startup period during which bulk flow quantities may evolve over time. The determination of convergence to steady state is usually at the discretion of the DSMC code user, and statistical scatter generally prevents residual tracking of the type often used to measure solution convergence in deterministic CFD simulations. This tends to result in a tradeoff between simulation efficiency and accuracy, as a more conservative estimate of the transient time interval reduces the probability of initiating sampling while the flow is still evolving, but may lead to unnecessarily high simulation expense.

Common techniques for estimating convergence to steady state in DSMC include tracking the time variation in the total number of simulated particles [2] or the total number of simulated collisions per time step. The transient period may also be estimated by calculating the approximate time for acoustic waves to pass through the simulation domain, then applying a safety factor which depends strongly on the type of flow being simulated [3]. An alternate technique, implemented in recent DSMC codes of Bird [4], involves comparison of normalized differences in the total number of particles over large time intervals to some fixed tolerance value. Yet another technique, for use when aerodynamic coefficients are the main output parameters of interest, compares net momentum and energy fluxes along external grid boundaries to the total force and total heat transfer acting on an immersed solid body [5]. While such techniques may often give a reasonably good estimate of the time required to reach steady state, resulting information must be judged with the above accuracy/efficiency tradeoff in mind, and determination of solution convergence can be regarded as one of the more difficult concepts for inexperienced DSMC users. Consideration of the total number of simulated particles or collisions may be particularly problematic when applied to flows involving large local variation in gas density, recirculating regions, or an isolated volume (such as a driven cavity or one dimensional channel flow) through which particles cannot enter or escape.

In this paper, a new global convergence parameter is proposed to quantify the maximum departure from steady state conditions over the full simulation domain. Compared to existing techniques for DSMC convergence detection, the new parameter should be more sensitive to temporal changes within small flowfield regions or within regions of relatively low density, and should function very similarly to CFD residuals in tracking solution convergence for a wide variety of flows. In the following sections, a new procedure for convergence detection is outlined, and underlying approximations and assumptions are described. The new procedure is then evaluated through comparison with existing

convergence detection techniques for a nozzle/plume expansion flow, a hypersonic flow around a cylinder, and a subsonic driven cavity flow problem.

## 2 Detection of convergence to steady state

As a starting point in procedures for global convergence detection, we intend to evaluate the maximum time variation in some local flow quantity throughout the simulation domain. A parameter based on this maximum variation should function similarly to the  $L$ -infinity norm commonly used in CFD calculations, but instead of approaching machine zero (to within a few orders of magnitude) to indicate a converged solution, the parameter should approach a larger value associated with expected levels of statistical scatter. Global convergence is then assumed once the parameter reaches this predicted steady state value.

In the proposed convergence detection technique, the parameter for global convergence detection is a function of the maximum local time variation in outward-directed number flux along the boundaries of the simulation domain. This local variation is evaluated through a comparison of fluxes over two successive time periods, by means of two integer variables  $N_1$  and  $N_2$  which are assigned to the data structure for each face (or, similarly, for each cell) along any external boundary of the computational grid. Any face comprising part of a wall, symmetry, inflow or outflow boundary will therefore be assigned these two variables. During particle movement operations performed at each simulation time step, the  $N_1$  value at a given face will be incremented by one for every particle that exits the simulation domain (for inflow or outflow boundaries) or collides with a wall or symmetry boundary along this face. After a time period corresponding to a large number of simulation time steps, values of  $N_1$  and  $N_2$  are compared at each boundary face to calculate a global convergence parameter  $Q$ , after which  $N_2$  is set to equal  $N_1$  and  $N_1$  is then reinitialized as zero. Thus,  $N_1$  and  $N_2$  represent the total number of particles with trajectories that intersect a boundary face over successive time periods. These periods should be long enough to capture any unsteady bulk motion in the flow, and longer periods tend to better indicate transient behavior due to reduced statistical scatter associated with larger values of  $N_1$  and  $N_2$ . A period on the order of 5000 time steps is recommended for most DSMC applications.

In order to determine an appropriate convergence parameter  $Q$ , we assume that all trajectory-face intersections which contribute to  $N_1$  are statistically independent and follow a Poisson distribution. The difference  $N_1 - N_2$  therefore has a Skellam distribution [6] with a variance of approximately  $N_1 + N_2$  and a mean value of zero at steady state. Thus, when steady state conditions have been attained along all boundary faces, the probability

$$P\left[\frac{|N_1 - N_2|}{\sqrt{N_1 + N_2}} < K\right]$$

should be nearly equal at each face for any positive constant  $K$ . If  $M$  is the total number of boundary faces for which both  $N_1$  and  $N_2$  are nonzero,  $i$  is the boundary face index, and

$N_A$  and  $N_B$  are two integers independently sampled from the same Poisson distribution with mean and variance  $\bar{N}$ , it follows that the approximation

$$P\left[\max_{i \in [1, M]} \left\{ \left( \frac{|N_1 - N_2|}{\sqrt{N_1 + N_2}} \right)_i < K \right\}\right] = \prod_{i=1}^M P\left[\left( \frac{|N_1 - N_2|}{\sqrt{N_1 + N_2}} \right)_i < K\right] \approx \left(P\left[\frac{|N_A - N_B|}{\sqrt{2\bar{N}}} < K\right]\right)^M \quad (2.1)$$

will be satisfied at steady state. Note in Eq. (2.1) that the variance of  $N_1 - N_2$  is the sum of the expected mean values of  $N_1$  and  $N_2$  and is not exactly equal to  $N_1 + N_2$ . Next we define  $K_{0.5}$  as a function of  $M$  such that

$$\left(P\left[\frac{|N_A - N_B|}{\sqrt{2\bar{N}}} < K_{0.5}(M)\right]\right)^M = 0.5. \quad (2.2)$$

By substituting  $K_{0.5}$  for  $K$  in Eq. (2.1), we can show that  $P[Q < 1] \approx 0.5$  if steady state conditions have been attained along all boundary faces, where

$$Q = \frac{\max_{i \in [1, M]} \left\{ \left( \frac{|N_1 - N_2|}{\sqrt{N_1 + N_2}} \right)_i \right\}}{K_{0.5}(M)}. \quad (2.3)$$

Thus, at steady state, the quantity  $Q$  will have a median value of approximately one. Transient behavior along any boundary face will result in increased values of  $Q$ , and this parameter can therefore be used to evaluate the maximum departure from steady state conditions throughout the simulation domain. In general, steady state can be assumed once the condition  $Q \leq 1$  (or, similarly,  $Q \leq 1 + \varepsilon$  for some small tolerance  $\varepsilon \ll 1$ ) has been satisfied.

As given in Eq. (2.3), evaluation of  $Q$  requires knowledge of the normalization value  $K_{0.5}$ , which satisfies Eq. (2.2). While it may be possible to find an exact expression for  $K_{0.5}$  by inverting the Skellam cumulative distribution function, the approximate nature of the proposed convergence detection technique allows us to calculate  $K_{0.5}$  with acceptable accuracy using a numerical correlation. One such correlation is found through the following procedure: two integers  $N_A$  and  $N_B$  are independently sampled  $10^7$  times each from a Poisson distribution with a mean  $\bar{N}$  of 100. Next, for each of 50 parameter values  $(K_{0.5})_j = [0.1, 0.2, 0.3, \dots, 4.9, 5.0]$  a corresponding variable  $P_j$  is set to equal the fraction of  $(N_A, N_B)$  combinations for which  $|N_A - N_B| < \sqrt{2\bar{N}}(K_{0.5})_j$  is satisfied. We then compute  $M_j = -\ln 2 / \ln P_j$  for all  $j \in [1, 50]$ .

For  $M_j > 20$ , the variation in  $K_{0.5}$  with  $M$  is found to be closely approximated by a correlation of the form

$$K_{0.5}(M) = \sqrt{a + b \ln(M)}, \quad (2.4)$$

where  $a$  and  $b$  are constants. From a least-squares curve fit, we find  $a = -1.23$  and  $b = 1.85$ . In Fig. 1, the trend line given by Eq. (2.4) is plotted against a line between data points  $(M_j, (K_{0.5})_j)$  from the direct probabilistic solution to Eq. (2.2). In observing Fig. 1, we find

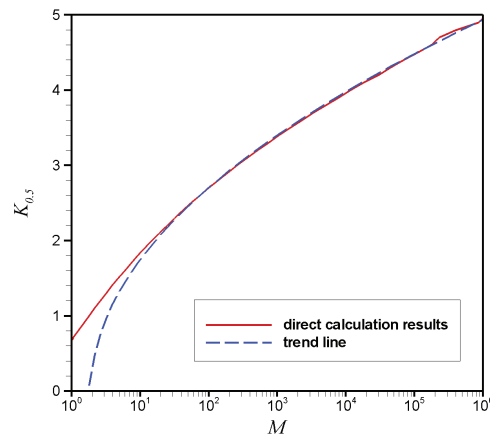


Figure 1: Variation in the normalization value  $K_{0.5}$  with the number of boundary faces  $M$ .

a high level of agreement between the two curves over nearly five orders of magnitude variation in  $M$ . Discrepancies between the two curves for  $M \gg 1$  are primarily due to statistical scatter. However, relatively poor agreement is found for small values of  $M$ ; the trend line underestimates  $K_{0.5}$  by approximately 2%, 5% and 31% for  $M = 20$ , 10 and 3 respectively, and the above values for  $a$  and  $b$  give no real solution to Eq. (2.4) if  $M = 1$ . Note that such very small values of  $M$  correspond primarily to homogeneous flow problems, and are unlikely to be encountered in most DSMC applications.

Also note that the effectiveness of the convergence parameter  $Q$  in assessing departure from steady state is subject to several assumptions: first, as described above, we assume that the sampling periods for  $N_1$  and  $N_2$  are not too short to capture unsteady characteristics at a given face due to either long transient time scales or excessive statistical scatter. Furthermore, we assume that unsteady characteristics at any point in the flow correspond to time variation in the unidirectional number flux along at least one boundary face. This implies that, as is generally the case, the region of slowest convergence is near some wall, symmetry, or inflow/outflow boundary. Finally, we assume that  $N_1$  and  $N_2$  follow a Poisson distribution, and that the mean value of  $N_1 - N_2$  will asymptotically approach zero at all boundary faces during convergence to steady state. This last assumption may be problematic in flows (such as those involving very long oblique shocks or shock-boundary layer interactions) which, as discussed below, potentially allow scatter-induced fluctuations in the location of shocks or other high gradient regions. In most cases, however, the use of a Poisson distribution to model the unidirectional flux of particles crossing a plane is an excellent approximation. As shown by Hadjiconstantinou et al. [7] through statistical mechanics arguments and through DSMC calculations, the Poisson distribution assumption is strictly valid at equilibrium, and is very accurate even under highly nonequilibrium conditions.

Given the above assumptions and limitations, the parameter  $Q$  is not proposed as a universal solution to the convergence detection problem for all DSMC simulations, but

instead as a reasonable balance between simplicity, efficiency, ease of implementation and fidelity for a range of simulation types. While consideration of variation in flowfield properties throughout the simulation interior (at each grid cell, for example) may seem like a more appropriate means of evaluating convergence, the use of boundary fluxes provides a number of advantages:

First, a relatively small number of values (the normalized difference  $|N_1 - N_2|$  at each boundary face) are compared in order to determine the maximum degree of unsteadiness throughout the simulated flowfield. By considering values which are only assigned to boundary faces, and not every cell in the grid, we increase sensitivity to any weak transient behavior by reducing the relative influence of statistical fluctuations. (Such increased sensitivity can be explained by the fact that, when a smaller number of values are compared, there is a reduced probability that the largest value will result from a large, improbable statistical fluctuation in  $|N_1 - N_2|$  at steady state.)

Second, summations over particle trajectory-boundary intersections, which are equivalent to time-averaged values of the unidirectional number flux, allow determination of normalized differences by means of only two integer variables per face. Other fluxes—particularly the total energy flux—may be more sensitive to unsteady phenomena in some DSMC simulations, but require more variables per face and more complicated normalization procedures.

Third, if necessary, the parameter  $Q$  can easily be modified to depend on only wall boundary faces. As discussed below, this modification may be appropriate in simulations of external flows around hypersonic vehicles, where aerodynamic data and surface heat transfer are the primary output quantities of interest, and where very small scatter-induced fluctuations in the bow shock can increase steady state  $|N_1 - N_2|$  values along farfield outflow boundaries beyond physically expected levels.

Finally, the use of flux quantities allows us to compute time-averaged values by summing over statistically independent contributions during every time step. Volume-based quantities—such as the density, bulk velocity or temperature in each cell—may at first seem like better candidates for examination of transient characteristics, and could allow such characteristics to be monitored throughout the simulation domain in a similar manner to CFD residual tracking. However, the desire to distinguish transient behavior from statistical scatter leads to a requirement that this scatter be quantified. When volume-based quantities are calculated using summations over multiple time steps (as is typically required to avoid excessive scatter) the associated statistical scatter is very difficult to determine, and is generally a strong function of the residence time for each particle within the sampling volume. For example, if a particle remains in a given cell over a large number of time steps, then this particle will have a comparatively large influence on the time-averaged cell density. As a result, some increase in statistical dependence is expected among contributions to the summation used to calculate density, and estimates of the density variance should account for this effect. In contrast, no significant statistical correlations are expected for time-averaged flux quantities, and determination of the variance due to scatter in these quantities is relatively simple.

### 3 Expansion flow simulation

As an initial test case to evaluate the proposed convergence criterion  $Q \leq 1$ , we consider the expansion of molecular nitrogen through a conical divergent nozzle into a vacuum. An axisymmetric simulation is performed using the DSMC code MONACO [8]. At simulation startup, the entire flowfield is initialized as a vacuum, and the variable hard sphere (VHS) model is used along with adaptive subcell procedures for collision partner selection [1]. Vibrational excitation is neglected, and a model of Boyd is used for rotational-translational energy exchange [9]. Inflow properties include a Mach number of 1.3 and a temperature of 500K, and the nozzle surface is modeled as a diffusely reflecting isothermal wall at 500K. The nozzle has a uniform divergence half angle of  $20^\circ$ , an area ratio of 80 and an exit diameter of 0.0036m. The nozzle is 3.9cm in length, and the simulation domain extends an additional 4cm downstream from the nozzle exit plane and 5cm radially outward from the central axis. Vacuum outflow boundary conditions are employed along the nozzle exit plane and along other grid boundaries within the plume region. The inflow density is  $0.014\text{kg/m}^3$ , which corresponds to an inflow Knudsen number based on local nozzle diameter of 0.0014 and a centerline Knudsen number of approximately 0.005 at the nozzle exit. The computational grid consists of 55,409 quadrilateral cells and 917 external grid boundary faces, with cell sizes roughly adapted to the local mean free path.

Fig. 2 shows the variation in the global convergence parameter  $Q$ , which is evaluated once every 5000 time steps, as a function of time step number over the course of the simulation. The total number of simulated particles is plotted for comparison. As shown in the figure, the number of particles rapidly increases during the first several thousand time steps after simulation startup, and reaches a plateau around  $8.22 \times 10^6$  at steady state. At step 25,000, the number of particles is within 2.2% of the time-averaged steady state value, and total particle populations are within 1% and 0.1% of this value at steps 30,000 and 40,000 respectively. In contrast, the value of  $Q$  is shown in Fig. 2 to vary between 17 and 37 during the first 25,000 steps, with a value of approximately 1.50 at step number 40,000. The convergence criterion  $Q \ll 1$  is not satisfied until step 50,000, after which the median value of  $Q$  is very close to one (indicated by the dotted line in Fig. 2) as expected at steady state. For additional comparison, the total number of collisions per time step and the mean energy per particle are plotted as functions of the time step number in Fig. 3. Both quantities are found to be less sensitive to transient behavior than the total number of particles; the number of collisions is within 1% of the corresponding steady state value at step 20,000, and the mean energy is within 1% of the steady state value at step 25,000.

A comparison of the four curves in Figs. 2 and 3 indicates that the convergence parameter  $Q$  exhibits far greater sensitivity to transient characteristics than other quantities commonly used to detect global convergence to steady state. As an additional advantage relative to the other quantities plotted in Figs. 2 and 3, the approximate median value of  $Q$  at steady state is known a priori. In contrast, steady state values of nearly any other rele-

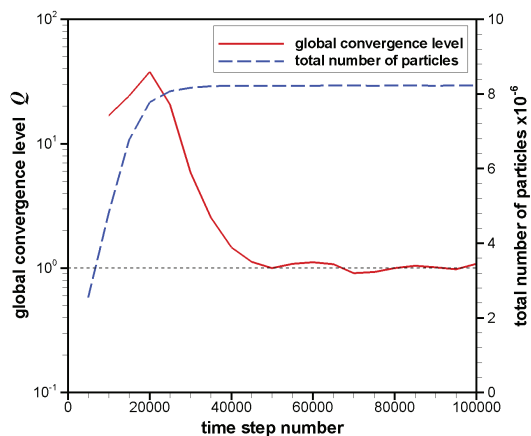


Figure 2: Time variation in the convergence parameter  $Q$  and the total number of particles.

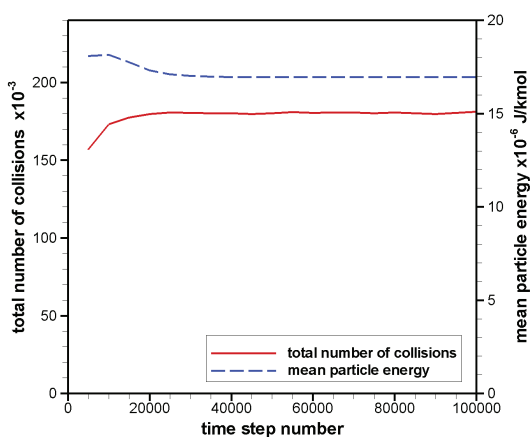


Figure 3: Time variation in the total number of collisions and the mean particle energy.

vant global value can usually be determined only from time-averaged simulation results. One further advantage of the parameter  $Q$  is that, by retaining the center coordinates of the face  $j$  for which

$$\left( \frac{|N_1 - N_2|}{\sqrt{N_1 + N_2}} \right)_j = \max_{i \in [1, M]} \left\{ \left( \frac{|N_1 - N_2|}{\sqrt{N_1 + N_2}} \right)_i \right\} \quad (3.1)$$

during each evaluation of Eq. (2.3), we can find the approximate location of maximum temporal variation during each summation period. Applying this procedure to the expansion flow problem, we identify the location of slowest convergence—where Eq. (3.1) is satisfied between steps 35,000 and 45,000—as the area furthest from the symmetry axis along the nozzle exit plane. Standard DSMC convergence detection techniques are expected to be particularly insensitive to transient characteristics in this area due to the

extremely low density, while convergence should be especially slow here as a result of the large relative distance from the nozzle inflow boundary.

The lack of a converged solution over a sampling period between time steps 40,000 and 45,000 is observed in Fig. 4, where density iso-contour lines are shown for this sampling period along with lines based on additional periods from step 50,000 to 55,000 and from step 50,000 to 100,000. Note that all density values in Fig. 4 are normalized by the stagnation density of  $0.029\text{kg/m}^3$ . As shown in the figure, excellent agreement is found in the region of slowest convergence between results from the latter two sampling periods, whereas the earlier sampling period gives noticeably lower densities in this region. At the point ( $x = 0\text{m}$ ,  $r = 0.05\text{m}$ ) the sampling period between steps 40,000 and 45,000 is found to underestimate the density by 6.6% relative to the steady state value (as taken from the 50,000 to 100,000 step sampling period) while a much smaller underestimate of 0.5% is found for the sampling period between steps 50,000 and 55,000. It follows that global steady state conditions can be safely assumed after 50,000 steps, as predicted by the convergence criterion  $Q \leq 1$ , but significant transient characteristics are observed at step number 40,000.

As an additional means of assessing convergence to steady state, we consider a modification to Eq. (2.3) based on the total number of particles in the grid. A new parameter  $\Delta$  is defined such that

$$\Delta = \frac{1}{K_{0.5}(1)} \frac{|\eta_1 - \eta_2|}{\sqrt{\eta_1 + \eta_2}}, \quad (3.2)$$

where  $\eta_1$  is the total number of particles during the current time step and  $\eta_2$  is the corresponding value at some previous time step. Assuming the time interval between these two steps is large compared to the mean particle residence time within the simulation domain,  $\eta_1$  and  $\eta_2$  may be treated as statistically independent Poisson distributed quantities. The variance of  $\eta_1 - \eta_2$  can therefore be approximated as  $\eta_1 + \eta_2$ . Similar reasoning to that used above for  $Q$  can be employed to argue that, at steady state,  $\Delta$  should have a median value near one. As found in Fig. 1, the normalization coefficient  $K_{0.5}(1)$  in Eq. (3.2) is approximately 0.676. Note that a very similar normalized difference  $|\eta_1 - \eta_2|$  is used in the DS2V DSMC code of Bird for automatic initiation of steady state sampling procedures [4].

In Fig. 5, the two convergence parameters  $Q$  and  $\Delta$  are plotted as functions of the time step number. The dotted line denotes expected median values at steady state for both  $Q$  and  $\Delta$ . While  $Q$  exhibits far less scatter at steady state than  $\Delta$ , the latter parameter varies over a larger range during the startup period. As with the condition  $Q \leq 1$ , the condition  $\Delta \leq 1$  is not satisfied until step number 50,000, which indicates a comparable sensitivity to local transient characteristics within a small, low density region. It should be emphasized, however, that the median steady state value of  $\Delta$  is known with considerably less certainty than that of  $Q$ , because any individual particles that contribute to both  $\eta_1$  and  $\eta_2$  tend to reduce the variance of  $\eta_1 - \eta_2$ . As a result, smaller time intervals used in the evaluation of Eq. (3.2) can lead to smaller values of  $\Delta$  at steady state. Although the relative

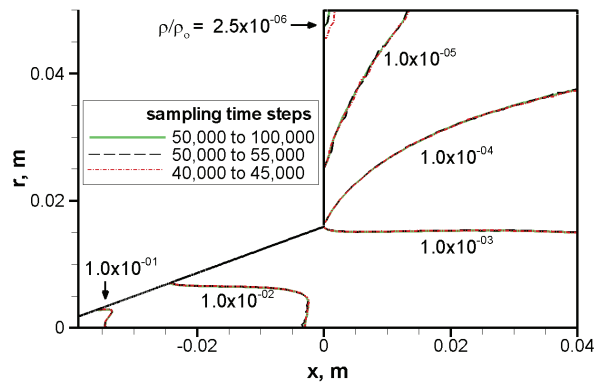


Figure 4: Normalized density contours based on three different sampling periods.

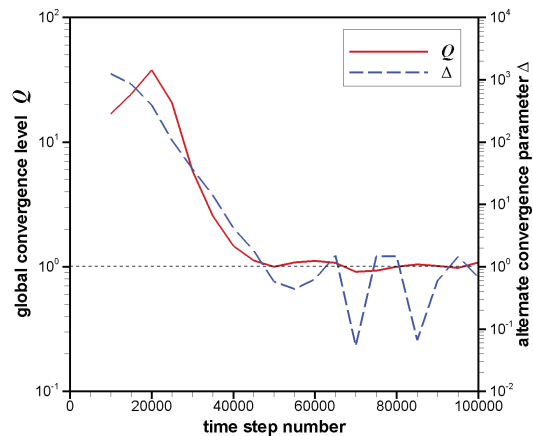


Figure 5: Time variation in convergence parameters  $Q$  and  $\Delta$ .

effectiveness of the two parameters  $\Delta$  and  $Q$  may be problem dependent, both increased scatter and reduced expectation accuracy at steady state should, in general, make  $\Delta$  a less reliable indicator of steady state conditions than  $Q$ .

## 4 Hypersonic blunt body flow

As an additional test case to evaluate the proposed convergence detection technique, we consider a two dimensional hypersonic flow of  $N_2$  over a cylinder. The freestream Mach number is 20, the Knudsen number based on cylinder diameter is 0.01, and the same numerical models and approximations are used as in the expansion flow simulation described above. The freestream temperature is 217.5K, the cylinder wall temperature is 1500K, and the wall thermal accommodation coefficient is 1.0. The computational domain extends 2.2 cylinder diameters downstream and 2.5 diameters outward from the cylinder

center, and the grid consists of 63,777 triangular cells refined everywhere to the local mean free path. Steady state Mach number contours and streamlines are shown in Fig. 6; note the well-defined bow shock and the small recirculation zone within the subsonic near-wall region of the wake.

Fig. 7 shows the time variation in the convergence parameter  $Q$ , as evaluated once every 5000 time steps based on only wall boundary faces or based on all faces along any external grid boundary. The total number of particles is also plotted for comparison. As shown in the figure, around step 25,000 the wall-based parameter  $Q$  reaches a plateau with a median value slightly greater than one, whereas the number of particles reaches a plateau approximately 5000 steps earlier. (Note, however, that the more stringent convergence criterion  $Q \leq 1$  is not satisfied until step number 50,000.) In contrast, the convergence parameter based on all boundary faces (the dotted line in Fig. 7) shows considerable scatter at steady state, with no clearly differentiated transient period. This surprising characteristic is found to result from very small fluctuations in the intersection point of the bow shock with an outflow boundary far from the symmetry axis. Such tiny fluctuations in farfield shock location are in turn likely caused by the stochastic nature of DSMC, combined with the relatively large distance between the cylinder and the outflow boundary.

Due to the effectiveness of the proposed convergence parameter  $Q$  in discerning this type of scatter-induced shock fluctuation, a  $Q$  value based only on wall boundary faces is recommended for hypersonic blunt body flow simulations. In this type of simulation, surface fluxes are typically the primary quantities of interest, so a convergence indicator based on surface fluxes seems particularly appropriate. The suggested modification is further justified by the fact that, as observed for the cylinder flow case, recirculating regions along the body surface tend to reach steady state more slowly than any other flowfield region. At step 20,000 in the cylinder flow simulation, when the number of particles is negligibly different than the time-averaged steady state value but the wall-based  $Q$  value is still greater than two, the location of maximum unsteadiness which satisfies Eq. (3.1) is, as expected, along the recirculation zone shown in Fig. 6.

Note that, although the recommended modification to  $Q$  for this type of flow may be implemented through a manual switch, a more user-friendly but less generalized automatic implementation can be used instead. In one possible implementation, this modification is triggered if the specified Mach number along all inflow boundary conditions is much greater than one.

In Fig. 8, variation in the heat transfer coefficient along the cylinder surface is shown for sampling periods between steps 20,000 and 22,500, steps 25,000 and 27,500, and steps 30,000 and 100,000. Results from the last sampling period are assumed to represent the steady state solution. Over much of the surface, differences observed between all three curves are comparable to the level of statistical scatter for the first two sampling periods. However, over the afterbody surface at angles greater than approximately  $150^\circ$ , noticeably better agreement with the steady state result is found for the period between steps 25,000 and 27,500. Results from both earlier periods are still observed in Fig. 8 to slightly

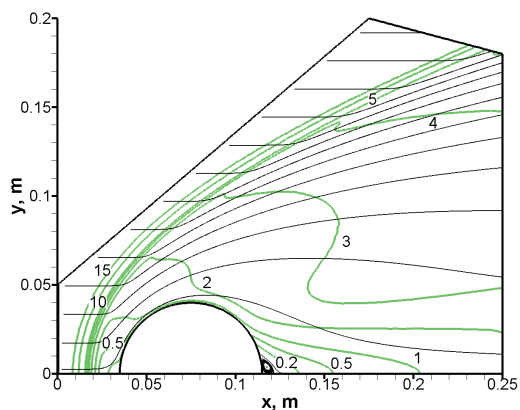


Figure 6: Mach number contours and streamlines for Mach 20 flow around a cylinder.

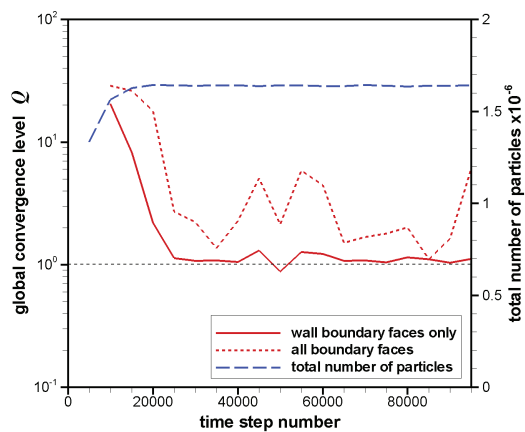


Figure 7: Variation in  $Q$  and in the total number of particles for the cylinder flow.

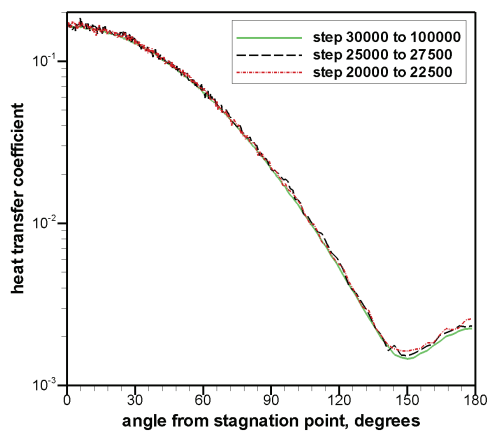


Figure 8: Heat transfer coefficient over the cylinder surface.

overestimate the surface heat transfer across this region. By comparison with Fig. 7, it follows that, for this simulation, the parameter  $Q$  based on wall boundary faces provides a more sensitive measure of unsteady characteristics than the total number of particles, but neither quantity shows desired sensitivity to a gradual change in afterbody surface heat transfer. However, as described above, we expect that the sensitivity of  $Q$  would increase if longer periods were employed for evaluations of this parameter. A longer evaluation period (e.g., 10,000 steps) could therefore be assumed to increase the number of time steps before  $Q$  first approaches the expected steady state median value of one.

## 5 Driven cavity flow

As a final representative test case to evaluate the new convergence criterion, an additional simulation is performed for a two dimensional subsonic driven cavity flow problem. In this simulation, initially quiescent nitrogen gas is contained within a square box of dimensions equal to 20 mean free paths, which corresponds to a global Knudsen number of 0.05. The initial gas temperature is 300K, and all boundaries are modeled as diffusely reflecting isothermal walls at this same temperature. At simulation startup, one wall boundary is impulsively accelerated in the wall-tangent direction to a Mach number of 0.5. A large subsonic recirculation zone then forms due to surface shear forces acting along the moving wall. The time step interval is approximately 0.2 times the gas mean collision time, the simulation domain is divided into  $20 \times 20$  square cells, and the particle numerical weight is set for an average of  $10^4$  particles per cell.

The very large number of particles per cell is used to compensate for otherwise excessively high scatter in simulation results based on time averages over the desired sampling period. In order to properly capture transient characteristics during the relatively short time to reach steady state, we use a period of only 100 steps for evaluation of the convergence parameter  $Q$ . Note that, if high resolution of transient characteristics were not required, a much longer evaluation period for  $Q$  could be used along with a far smaller number of particles per cell.

Fig. 9 shows the variation in  $Q$  over the course of the simulation, and the total number of simulated particles is also plotted for comparison. As the grid contains no inflow or outflow boundaries, the total number of particles is fixed at simulation startup and therefore cannot be used to detect convergence. Similarly, the total number of collisions per time step and the mean energy per particle are both found to vary by well under 1%, and both quantities provide little sensitivity to unsteady characteristics in this type of subsonic flow. In contrast,  $Q$  values in Fig. 9 indicate considerable unsteadiness during the first few hundred time steps, with rapid convergence to the expected median steady state value around one. The condition  $Q \leq 1$ , which is assumed to signify global convergence to steady state, is first satisfied at step number 800.

Fig. 10 shows contours of Mach number based on time-averaged sampling over the periods from step 400 to 500, step 800 to 900, and step 800 to 3000. Discrepancies between

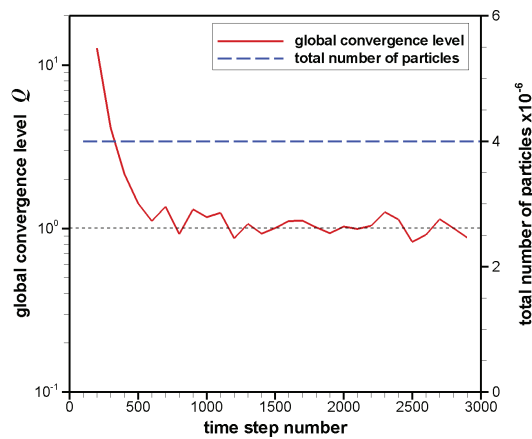


Figure 9: Variation in  $Q$  and in the total number of particles for a subsonic driven cavity flow.

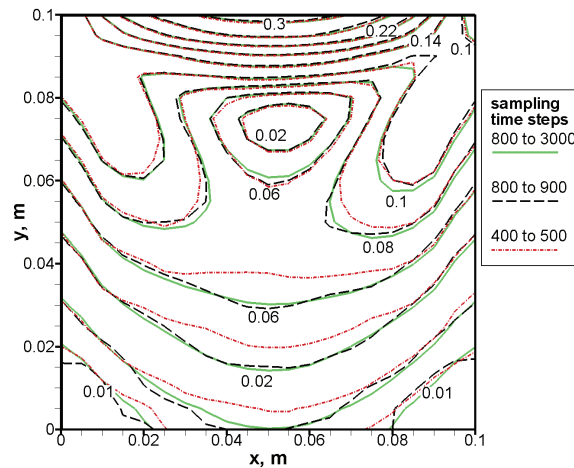


Figure 10: Mach number contours based on three different sampling periods.

contour lines from the latter two periods are generally within the observed level of statistical scatter. Thus, if the third sampling period is assumed to represent the steady state solution, then conditions during the second period, between steps 800 and 900, can also be assumed to represent steady state. However, much larger differences from the steady state solution are displayed in results for the first sampling period, between steps 400 and 500. In particular, during this earlier period, considerably reduced Mach number values are found far from the moving wall (at  $y = 0.1\text{m}$ ) which indicates a lack of fully developed recirculation. Trends observed in Fig. 10 seem to agree well with those in Fig. 9, and reinforce the conclusion that significant transient characteristics are present around step 400 but not around step 800.

## 6 Conclusions

A new technique for assessing global convergence to steady state in DSMC simulations has been presented. Relative to other DSMC convergence indicators, the proposed convergence parameter  $Q$  should generally provide increased sensitivity to weak transient characteristics in small regions of the simulated flowfield. Other advantages of the new technique include simple implementation, negligible impact on simulation expense or memory requirements, a priori knowledge of the expected median parameter value at steady state, and the ability to determine the area in the flowfield domain of slowest convergence. These characteristics of the new technique have been demonstrated for an expansion flow through a divergent nozzle into a vacuum, a hypersonic flow around a cylinder, and a subsonic driven cavity flow. An additional parameter based on the total number of simulated particles has been shown to provide comparable results for the expansion flow, but is subject to increased scatter and greater uncertainty in the expected median value at steady state.

It should be emphasized that the parameter  $Q$  is not proposed as a universal indicator for global convergence in all DSMC simulations of steady state flows. Instead,  $Q$  is intended as an easily computed and more sensitive alternative to global quantities, such as the number of particles or the number of collisions per time step, which are often used for convergence detection in DSMC. As described above, the technique presented here does have significant faults and limitations, including an assumption that the region of slowest convergence is close to an external grid boundary, and a minor modification required for application to hypersonic blunt body flow simulations. Still, this technique should hold promise as a simple means of reliably predicting steady state convergence for a wide range of DSMC simulations. Improved reliability in convergence detection can in turn reduce user input requirements through increased automation of DSMC numerical procedures. In addition, a reliable indicator of the time to reach steady state may allow improvements in either efficiency or accuracy, as uncertainty in this time typically leads to either unnecessarily long startup periods or accuracy loss due to a lack of convergence at initiation of time-averaged sampling routines.

## Acknowledgments

The authors gratefully acknowledge NASA for financial support of this work, through grant NNX08AD02A.

## References

- [1] G. A. Bird, *Molecular Gas Dynamics and the Direct Simulation of Gas Flows*, Clarendon Press, Oxford, 1994.

- [2] I. D. Boyd, Direct Simulation Monte Carlo for Atmospheric Entry Part I: Theoretical Basis and Physical Models, Hypersonic Entry and Cruis Vehicles, von Karman Institute for Fluid Dynamics, Rhode-Saint-Genese, Belgium, 2008.
- [3] M. A. Rieffel, A method for estimating the computational requirements of DSMC simulations, *J. Comput. Phys.*, 149 (1999), 95–113.
- [4] G. A. Bird, The DS2V/3V program suite for DSMC calculations, rarefied gas dynamics: 24th International Symposium, American Institute of Physics, 2005, 541–546.
- [5] D. F. G. Rault, Aerodynamic characteristics of a hypersonic viscous optimized waverider at high altitudes, *AIAA Paper*, (1992), 92-0306.
- [6] J. G. Skellam, The frequency distribution of the difference between two Poisson variates belonging to different populations, *J. Roy. Statist. Soc.*, 109 (1946), 296.
- [7] N. G. Hadjiconstantinou, A. L. Garcia, M. Z. Bazant and G. He, Statistical error in particle simulations of hydrodynamic phenomena, *J. Comput. Phys.*, 187 (2003), 274–297.
- [8] S. Dietrich and I. D. Boyd, Scalar and parallel optimized implementation of the direct simulation Monte Carlo method, *J. Comput. Phys.*, 126 (1996), 328–342.
- [9] I. D. Boyd, Analysis of rotational nonequilibrium in standing shock waves of nitrogen, *AIAA J.*, 28 (1990), 1997–1999.